Laboratory Demonstrations of Multi-Object Adaptive Optics in the visible on a 10 meter telescope

S. Mark Ammons*[a], Luke Johnson[a], Edward A. Laag[b], Renate Kupke[a], Donald T. Gavel[a]
[a]Center for Adaptive Optics, University of California, Santa Cruz, 1156 High St., Santa Cruz, CA USA 95060;
[b]University of California, Riverside, 900 University Ave., Riverside, CA USA 92521

ABSTRACT

We have demonstrated MOAO-type atmospheric compensation on a 10 meter telescope at visible wavelengths with the UCO/Lick MCAO/MOAO testbed in the Laboratory for Adaptive Optics at UCSC. We report Strehls of ~20% in R band (658 nm) on-axis and Strehls of ~15% off-axis 25" for a 3D Mauna Kea-type atmosphere with r_0 = 15 cm and θ_0 = 3.5". We show that a tomographic MOAO approach with 5 LGS's in a 50" constellation is sufficient to realize good correction in the visible. Two major improvements to the testbed realized this gain: (1) An upgrade to 64x64 subapertures across a 10 meter pupil (2) and a predictor-corrector wind model. We discuss limitations to wide-field visible light AO on 8-10 meter class telescopes and stress that the tomographic error due to blind modes is frequently the largest field-dependent error. We use a predictor-corrector wind model (Wiberg et al. 2006) to take advantage of wind-layer shearing in the atmosphere to reduce the tomographic error over a 50" diameter field. Depending on the validity of the Taylor frozen flow model for individual layers in the real atmosphere, this approach could be more effective than increasing the number of LGS's.
Keywords: multi-conjugate, multi-object, adaptive optics, deformable mirror, Shack-Hartmann wavefront sensor, woofer, open-loop, tomography, wind, Taylor frozen flow

1. INTRODUCTION

In recent years, demand for diffraction-limited imaging and spectroscopy from the ground over the medium field (0.5 – 2.0 arcminutes) has increased. The James Webb Space Telescope purports to deliver this quality of imaging as well as integral-field unit (IFU) type spectroscopy redder than 2 microns with a 6.5 meter aperture. The superb Hubble Space Telescope will be refurbished in 2008 with the Wide Field Camera 3 (WF3) as well as other new instruments, giving images with full width at half max (FWHM) between 35 and 150 millarcseconds from the optical to H-band. The coverage of the wavelength/spatial resolution plane provided by these two facilities is a great step forward, but further coverage can be provided with near-IR adaptive optics (AO) on 8-10 meter class telescopes and visible light AO on 3-6 meter class telescopes. Although much science has been performed with the narrow-field capabilities of existing near-IR AO systems at 30-50% Strehl, pushing to wider field (0.5 – 2.0 arcminutes) will enable survey capabilities that will complement existing diffraction-limited facilities.

1.1 Multi-conjugate and Multi-Object adaptive optics

Multi-conjugate[1] and Multi-Object[2,3,4] Adaptive Optics (MCAO and MOAO) are two proposed technologies that will deliver corrected wavefronts over these desired fields of view. MCAO has recently been demonstrated on the sky with natural guide stars (NGS)[5], and Gemini-South is nearing completion of a laser guide star (LGS) MCAO system. MAD's deliverance of 20-40% Strehl across a 2 arcminute field with 3 bright natural guide stars has increased confidence in this technique, and many more on-sky MCAO systems have recently entered the design and construction stage, both for extremely large telescopes (ELTs) and 8-10 meter class telescopes. In addition, MCAO has been demonstrated in the laboratory and on-sky for solar adaptive optics.[6,7]

*ammons@ucolick.org; phone 1 831 459-1637; fax 1 831 459-5717; cfao.ucolick.org

Adaptive Optics Systems, edited by Norbert Hubin, Claire E. Max, Peter L. Wizinowich,
Proc. of SPIE Vol. 7015, 70150C, (2008)
0277-786X/08/$18 · doi: 10.1117/12.790188

MCAO and MOAO refer to different methods of adaptive optics correction, but wavefront sensing is performed in a similar manner for both, via individual wavefront sensors looking at individual stars (star-oriented wavefront sensing, SO). Layer-oriented wavefront sensing (LO) is an alternative method of wide field sensing that optically combines guide star light at different turbulent layers in the atmosphere,[8] a concept that is currently being tested with pyramid wavefront sensors with the MAD on-sky demonstrator. Despite the method of correction (MCAO or MOAO) and the exact method of wavefront sensing (SO or LO), all require multiple guide stars distributed over a wide field.

MCAO systems deliver a wide, contiguous field of view by simultaneously correcting all layers of turbulence over some range of angles. This involves conjugating multiple deformable mirrors to different atmospheric layers and "collapsing" the three-dimensional atmosphere onto these planes. MOAO systems split the focal plane into multiple beams and apply optimized corrections to the pupil planes formed in each beam. The deformable mirrors used in MOAO systems to apply these corrections are all optically conjugate to the ground. The wavefront sensors must pick off the laser guide star beams, which do not propagate into the deformable mirror paths (the multi-object "arms") because the LGS footprint in the focal plane is much larger than the pick-off mirrors for the arms. For this reason, the wavefront sensors and the deformable mirrors are optically separate. This prevents closed-loop operation in the traditional sense and necessitates operation in open-loop.

Several MOAO testbeds and integrated demonstrators exist, including the SESAME bench at Observatorie du Paris (Rousset, this conference), meant to provide wide-field correction in K-band on an 8-meter telescope. Although several key MOAO concepts have been demonstrated on-sky (open-loop operation of wavefront sensors[9] and atmospheric tomography[10]), a fully integrated system of multi-GS wavefronts sensors, tomographic analysis, and single-DM correction has not been performed on-sky. The CANARY[11] demonstrator for the E-ELT will likely be the first. The Next Generation Keck Adaptive Optics system[12,13] (NGAO) will be the first facility-class science instrument that takes advantage of tomographic analysis of a multi-layer atmosphere.

1.2 Tomographic analysis of atmosphere

The observable wavefronts in multi-guide star wavefront sensors are the integrals along a 3-D volumetric atmosphere along different lines-of-sight. A tomographic algorithm[14,15] can be used to directly compute the phase in metapupils at various heights through the atmosphere from these integrated wavefronts. In MOAO, the deformable mirror correction is intended to be optimized along a single line of sight through the 3-D atmosphere. This desired phase can be computed via another line integral through the tomographically reconstructed layers of atmosphere along a specified direction. Because the phase correction is performed with one deformable mirror conjugate to the ground, the correction can be optimized for that direction, while other directions are subject to classic anisoplanatism error. Nominally, other MOAO arms with other deformable mirrors optimize corrections in other directions, allowing for multi-object capabilities. MOAO systems do not see the generalized anisoplanatism error term, present in MCAO systems, which is due to the inadequacy of multiple planar deformable mirrors to correct a three-dimensional volume of phase aberration.

Although the aim of MOAO may be to extend good correction to a wider field, the use of tomography to gain full knowledge of the atmospheric distribution can be used to correct the cone effect, or focal anisoplanatism, which is inherent to laser guide star AO (LGSAO) systems. This error term is present because the cone of atmosphere sampled by the laser guide star does not overlap sufficiently with the cylinder of turbulence sampled by an object at infinity. For this reason, AO systems that use laser tomography (LTAO) systems may reach higher Strehl on-axis than traditional LGSAO systems of equivalent subaperture size, correction rate, and total laser brightness. However, tomographic analyses experience another type of error called the "tomographic error." Assuming that the positions of the multiple laser guide stars are well-known, and additionally that there are no regions of turbulence that are entirely unsensed by the multiple guide stars, this error term refers only to "blind modes" of turbulence. The blind modes are three dimensional modes that are unsensed due to the geometry of the LGS constellation. The power spectrum of the blind modes depends on the orientation and the repetition of frequencies in the constellation; an LGS constellation of small radius (20" diameter for a 10 meter telescope) produces more power in the high frequency blind modes and vice versa.

It must be stressed that this error term is a roadblock to wide-field visible light adaptive optics on 8-10 meter class telescopes. The tomography error is strongly dependent on LGS number. For 2 arcminute constellations with 5-10 laser guide stars, the tomographic error is still on the order of 80 nm RMS for distant stars, which prevents off-axis Strehls

better than 15% in V-band under the best conditions (assuming measurement and fitting errors associated with a 64x64 DM, 50 W lasers, and no other error term).

1.3 Addressing tomography error with wind prediction

Wind prediction[16,17] and optimal Kalman filtering[18] hold great promise for reducing the effects of photon (measurement) error. Under the Taylor frozen-flow hypothesis, the atmospheric disturbance is unchanged temporally, but only shifted spatially from iteration to iteration. In principal, a single shifted measurement is sufficient to correct the atmosphere for the persistence time of the wind, allowing multiple measurements to be shifted and coadded, increasing signal-to-noise. The utility of these methods depend on the validity of the frozen-flow hypothesis for the atmosphere and the ease of isolating individual shear layers from integrated wavefront sensor measurements.

The application of wind prediction to multi-LGS tomographic systems allows for three key advantages. First, breaking the atmosphere into layers by height will separate uncorrelated shear velocities not by temporal, predictor-type analysis, but by purely geometric tomography. Predictor analysis can be applied to each reconstructed layer, increasing signal. Second, photons are a rare commodity in a multi-GS unit, either because multiple LGS's are expensive or because bright natural guide stars are rarely associated on the sky. Decreasing the effects of photon error with predictor/corrector methods by even a modest amount represents a substantial reduction in cost.

The third and most significant effect of wind prediction on a LTAO/MOAO system is a reduction of the tomographic error due to blind modes. These blind modes are three-dimensional, meaning that they have extent in atmospheric height in addition to spatial x-y. The natural shearing of wind layers in the atmosphere breaks the degeneracies that cause these errors. The "persistence distance," or the characteristic distance that wind travels before the Taylor frozen-flow hypothesis breaks down, would define the minimum frequency of the blind modes that can be measured utilizing predictor/corrector techniques. The best case scenario is an infinite persistence distance for all layers, providing attenuation of the error due to blind modes at all measurable frequencies.

1.4 Goals of this paper

In this paper, we mean to use the MCAO/MOAO testbed at the Laboratory for Adaptive Optics (LAO) at the University of California, Santa Cruz (UCSC) to demonstrate key technologies that enable precision MOAO correction on 8-10 meter class telescopes. This testbed, described in the next section, is a mock-up of a 10 meter telescope with multiple high-order deformable mirrors, wavefront sensors, and laser guide stars over a configurable constellation. We test the concept that temporally shifting-and-adding the atmosphere layer-by-layer may reduce tomography error due to blind modes. We use this concept to show that an LTAO/MOAO system on a 10-meter telescope may provide good correction at visible wavelengths (658 nm) both on- and off-axis for an atmosphere with $D/r_0 = 46$. A result of this experiment is an estimate of the high-altitude Taylor frozen-flow persistence distance required for noticeable improvement.

2. LAO MCAO/MOAO TESTBED

The LAO Multi-Conjugate/Multi-Object Adaptive Optics testbed is an integrated, multi-LGS tomographic unit executing wide-field adaptive optics atmospheric compensation on a three-dimensional, moving atmosphere with a 10 meter telescope. The testbed is meant to be modular, and has several movable deformable mirror ports, multiplexed Shack-Hartmann wavefront sensors, a wide-field science camera, configurable laser guide star constellations, and a variable sized telescope. The detailed layout of this testbed is described in previous publications.[19,20,21] We use three Hamamatsu X8267-16 Programmable Phase Modulators (PPMs) as deformable mirrors, with 768x768 pixels. Recently added is an ALPAO DM-52 woofer mirror, with magnetic actuation and up to 100 microns of stroke. Up to eight guide star Hartmann patterns can be imaged on two Dalsa 1024x1024 12-bit cameras, with pupils steered via a focal-plane quadcell, providing 100x100 subaperture capabilities with 4x4 pixel subapertures. The laser guide stars are simulated with multiple LEDs ($\lambda = 658$ nm) in a machined aluminum plate. A constellation of laser point sources at infinity, split from a 658 nm Crysta double YAG diode laser, is used to check Strehl over a wide field. This constellation of natural guide stars is imaged onto a Dalsa 1024x1024 12-bit camera. An image of the testbed layout is in Figure 1.

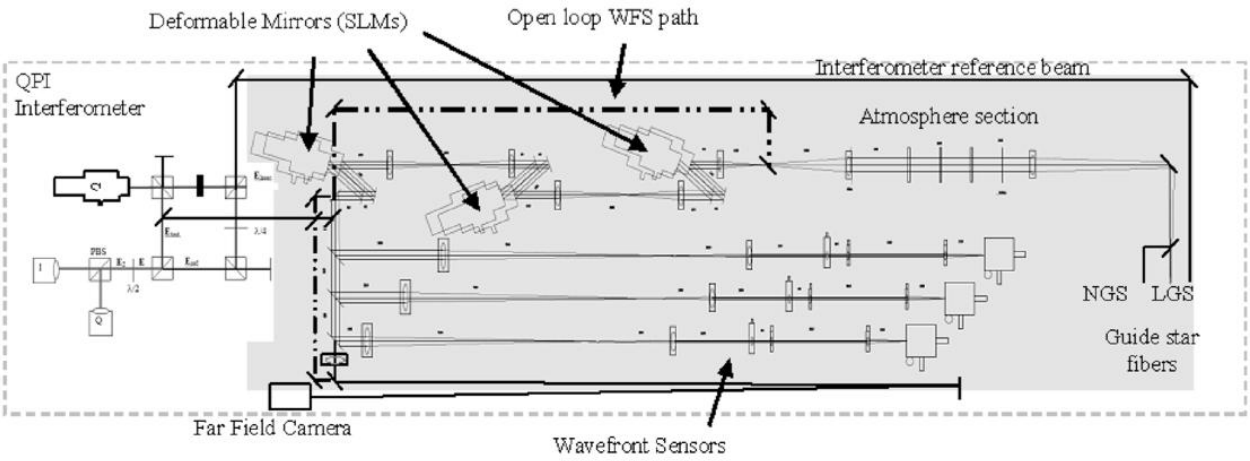

Fig. 1. Layout of the LAO MCAO/MOAO testbed. The open-loop WFS path, meant to enable quick simulation of open-loop operation, is not operational. We simulate open-loop operation by flattening all deformable mirrors before taking wavefront data.

2.1 Previous work with the MCAO/MOAO testbed

We have previously presented a characterization of the MOAO performance of the system for a 85 arcsecond diameter constellation at a science wavelength of 900 nm.[20] The LGS constellation had 5 stars in a "quincunx" (box-five) pattern and the Hartmann sensors had 36 subapertures across a 10 meter pupil. We assembled a complete error budget with terms measured independently via interferometric methods. This error budget was used to derive the tomography error, which was consistent to ~30% with the value predicted by simulations. The tomography error was derived by measuring the corrected Strehl with all atmosphere at the ground and comparing this to the Strehl with an MOAO-type correction on a three-dimensional atmosphere of the same magnitude. The tomography error was predicted to range between 75 nm on-axis and 95 nm at 60" for this constellation, and the measured values are ~100 nm for on-axis points and 125 nm at 60". The on-axis MOAO Strehl for this case is 36% on axis and 20-25% Strehl 60" off-axis.

The MCAO/MOAO bench has been used to demonstrate open-loop operation of wavefront sensors. In Ammons et al (2007), we show that open-loop accuracies of 30 nm RMS on atmospheres of 700 nm RMS can be reached with careful calibration. In this case of the MOAO 36x36 wavefront sensors, we calibrated the linearity of the device by raster scanning the laser guide star constellation in x and y in front of the AO system, recording the Hartmann signals, and inverting the signals to form a lookup table of linearized Hartmann slopes. The open-loop error is measured by comparing the wavefronts measured by 5 LGS's on a common ground layer.

The testbed has been used in MCAO mode[21] to demonstrate closed-loop stability of pseudo open-loop control[22] (POLC). With a multi-layer atmosphere in which the deformable mirrors are not conjugate to the dominant layers, the Strehl was shown to be improved and anisoplanatism suppressed with formulas in Tokovinin et al (2005).[23]

2.2 SLM wrapping and woofer mirror

A cursory summary of deformable mirror capabilities is presented here, but more detailed accounts are in previous publications.[19,20] The PPM deformable mirrors are optically addressed spatial light modulators (SLM) that have the capacity to modulate the phase of linearly polarized light at high spatial resolution. The light is polarized at the telescope with a 50.8 mm linear polarizer. The PPMs have a limited stroke of 800 nm at the center of the device and 650 nm near the edge. The effective stroke may be increased by wrapping phase, or making phase jumps at the contours of 2π radians. Monochromatic light is largely blind to these phase jumps, so PSF formation is unaffected. The SLMs are flattened during MOAO open-loop simulations, so wavefront sensing is not affected by the phase jumps.

An ALPAO DM-52 has recently been added to the optical conjugate to the ground layer. This mirror can be controlled to 10 nm RMS in open-loop.[24] It is used in this experiment to form static corrections for multiple field positions with no

atmosphere present, but it is not used to correct atmospheric distortion. Other in-lab experiments with MCAO indicate that the DM-52 is a stable woofer when combined with the SLM as a tweeter.[16]

2.3 Laser guide star elongation

The laser guide star constellation is mechanically elongated by shifting the LGS mount along the optical axis by 120 mm. Because geometric angles are magnified with respect to on-sky angles, this relatively large shift in height corresponds to an elongation of 0.6 Hartmann pixels (or one spot size of 2.0 arcseconds). An image of the elongated spots is in Figure 2. The photon error in this bench is small (10 nm RMS across a 10 meter pupil), so LGS elongation does not reduce the S/N of the wavefront sensor; in fact, by expanding the small Hartmann pixels, they improve the linearity and overall open-loop precision.

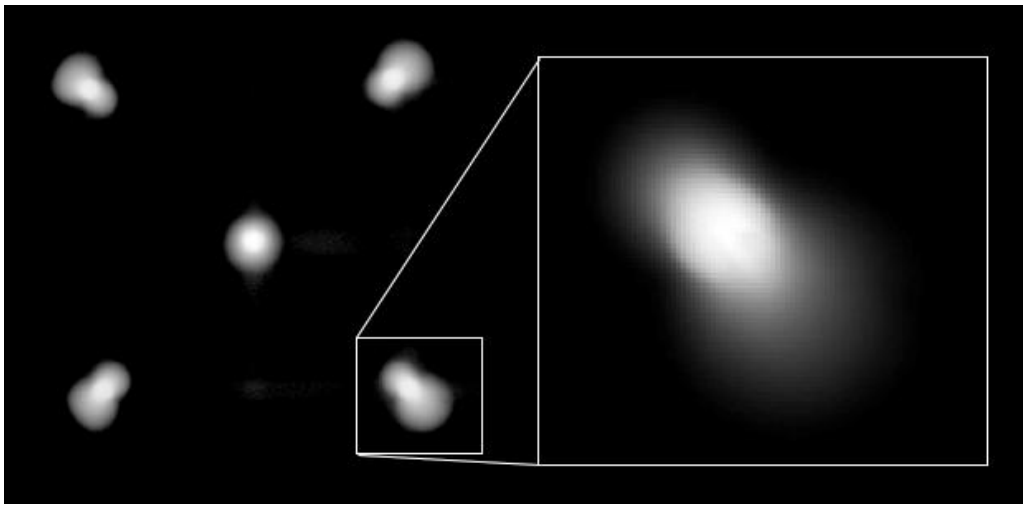

Fig. 2. Focal plane image of elongated laser guide star spots (using entire pupil). The characteristic peanut shape is present for side guide stars because the primary effect of shifting the LGS constellation along the optical axis is to defocus the guide stars (geometric ngles are demagnified with respect to on-sky angles).

2.4 Further details on MOAO implementation

We describe system parameters and methods relevant to the experiment, but refer the reader to Ammons et al (2007) for complete information on software, control, and other computational techniques. We use a simple 4x4 center of mass centroider without thresholding or windowing. Slopes are converted into full 64x64 wavefronts with an iterative Fourier transform-based reconstructor. The wavefronts are depistoned, detilted, dewarped, and analyzed with Tomography Spherical Wave.[14] This code is a minimum variance PCG solver utilizing back-propagation techniques and Kolmogorov post-filtering. Following tomographic analysis, the integrated phase in the direction of the science star of interest is computed and applied to the deformable mirror. After the science image is recorded, the forward propagation and Strehl check is repeated for all other science test stars.

A multiplicative gain must be applied to the forward-propagated wavefronts before the deformable mirrors are actuated. The Hartmann centroids are converted into physical slopes (nanometers of lift across a subaperture) by division by the Hartmann spot size, which is empirically measured. As a result, the final reconstructed wavefront is in units of nanometers. In the experiment that follows, a multiplicative gain of unity empirically produces the best Strehls.

System registration is accomplished by placing 25 Gaussians on the ground-layer SLM and recording the positions on the Hartmann sensor. Measured wavefronts are dewarped using this registration information with IDL's *warp_tri* function. Static corrections are generated for each field position by placing different order zernike modes on the woofer DM and maximizing (through a dithering technique) the image concentration in one λ/D diameter. When performing MOAO, the static correction appropriate to a particular star is used when checking Strehl on that star.

3. VISIBLE LIGHT MOAO EXPERIMENT

We now present an MOAO-type experiment that illustrates the reduction of tomography error occasioned by wind correction. This experiment includes 40 adaptive optics iterations, corresponding to a time length of 40 milliseconds if the correction rate is 1 kHz. We do not simulate bandwidth or delay error.

3.1 Experimental Setup

The MCAO/MOAO bench is configured with 64x64 subaperatures across a 10-meter telescope. The LGS constellation is shown in Figure 3. The 5 LGS's are arranged in a "quincunx" constellation, with natural test stars at infinity spread within the asterism.

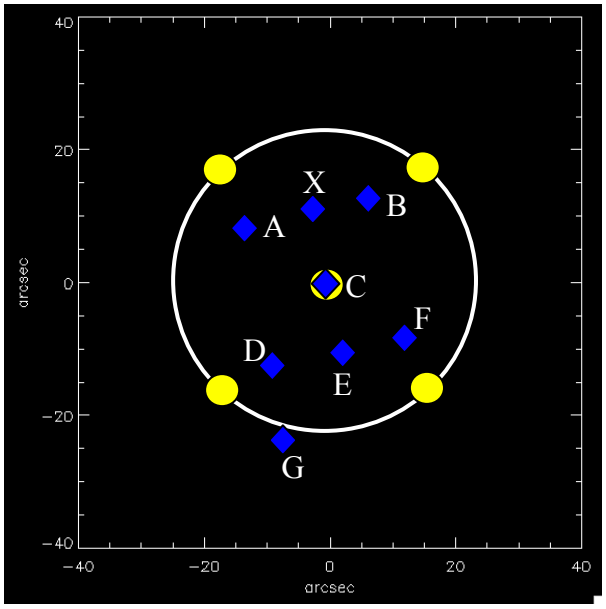

Fig. 3. Laser Guide Star constellation and positions of natural stars at infinity. The circle is 23" in radius. Yellow circles denote laser guide stars and blue diamonds denote natural test stars.

The atmospheric turbulence is distributed in 3 layers: 0 km, 4.5 km, and 9 km. The ground layer is by far the strongest, with 780 nm RMS of error. The middle layer has 320 nm RMS of error and the highest altitude has 90 nm. The total measured atmospheric strength is 940 nm RMS, which gives r_0 = 15.5 cm at 500 nm for a ten meter telescope (D/r_0 = 46.5). This defines θ_0 = 3.4" at 500 nm. The ground layer is set to flow North at 9.5 m/s, the middle layer South at 19 m/s, and the upper layer North at 41 m/s.

For each adaptive optics iteration, the LGS wavefronts are measured in open-loop (with the DMs flattened) and processed as in section 2.4. The atmospheric volume is reconstructed over three layers with the correct distribution of heights. The wavefronts that are forward-propagated for each test star are applied to the PPM (with the corresponding static correction on the woofer mirror) sequentially, with science camera exposures interleaved. This type of open-loop iteration is repeated 40 times, simulating 40 ms of AO operation with 1 kHz correction rate.

Wind correction is performed on a layer-by-layer basis, on tomographically reconstructed phases, not measured wavefronts. Layers reconstructed in previous AO iterations are shifted according to the known wind velocity and added with the current reconstructed layer. The gain is such that any iteration sees 30% of measured turbulence and 70% of shifted turbulence measured in previous iterations.

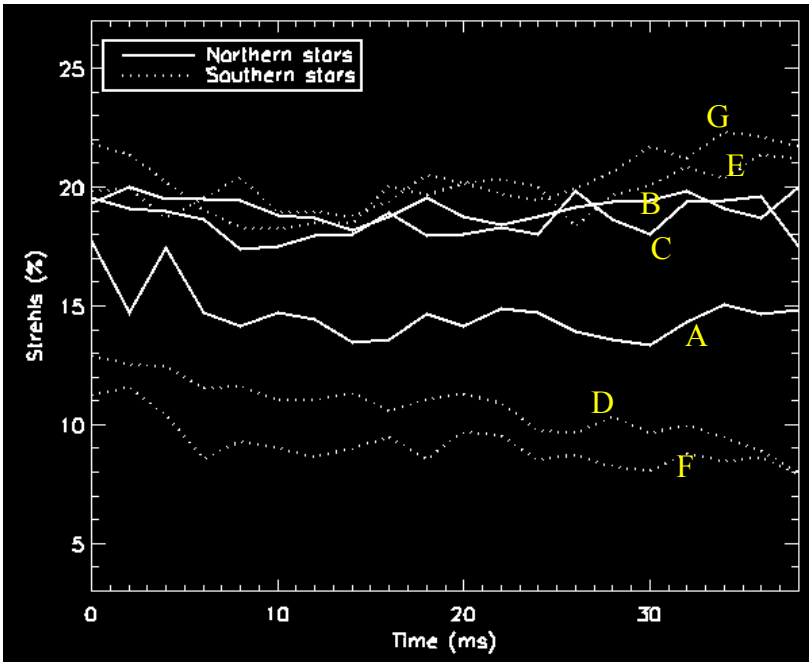

Fig. 4. Strehls for 7 test stars as a function of time. Not shown are absolute Strehls for star X, which are believed to be abnormally high (40%) due to hot pixels on the camera chip.

3.2 Results

All test stars see appreciable Strehl for this 40 ms experiment, with wind correction, as seen in Figure 4. The Strehls are quite non-uniform with position, which is likely a product of the fact that the simulation is short and that more atmospheric realizations are needed. The dominant ground layer has only a total shift distance of 1.2 subapertures, for example, and is largely unchanged through the simulation.

Most strikingly, an improvement is seen in the Strehls when wind correction is performed relative to the case without wind correction. As shown in Figure 5, the ratio between the Strehls for these two cases rises sharply to an average of 18% improvement for all test stars. The Northern stars are leeward for the highest altitude layer and see a greater average improvement of ~30% over 40 ms. The Southern stars are windward for the highest altitude layer, and see a smaller overall improvement of 10%.

Figure 6 displays the tomographically reconstructed layers of turbulence on the final iteration, both for wind correction and without. In the case without wind correction, there is a clear abundance of tomography error in a ring bordering the edge of the central metapupil. Notice that the structure within the metapupil sampled by all LGS's (inner ~50 subapertures) is different for both cases at the two higher altitudes, suggesting that some change to the reconstruction was made by the wind correction. In addition, the ring of tomography error surrounding this region at 9 km is suppressed at the bottom and top ends of the pupil, owing to a shifting of well-measured data into these regions over time.

Improvement is seen in as little as 10-20 iterations, which corresponds to a shift of 2.5-5 subapertures (or 0.4-0.8 meters) for the highest velocity wind layer and 0.2-0.4 meters for the medium layer.

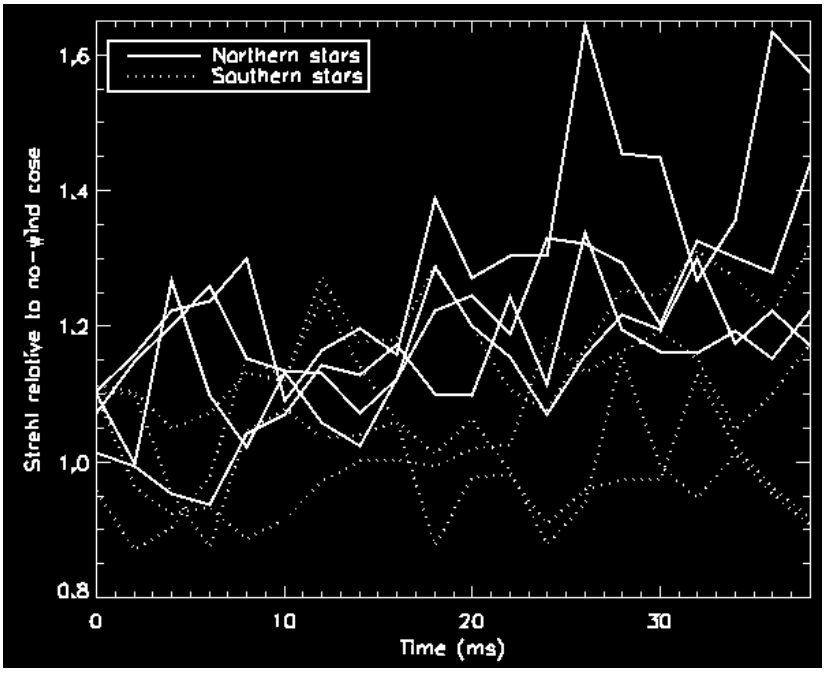

Fig. 5. Ratios of Strehls with wind correction to Strehls without wind correction, divided star by star, as a function of time. Notice that the Northern stars, which are leeward for the highest-altitude layer, see nearly 30% average improvement relative to the no wind correction case. Even the Southern stars, which are windward for the highest-altitude layer, see improvement due to wind shear of the middle layer.

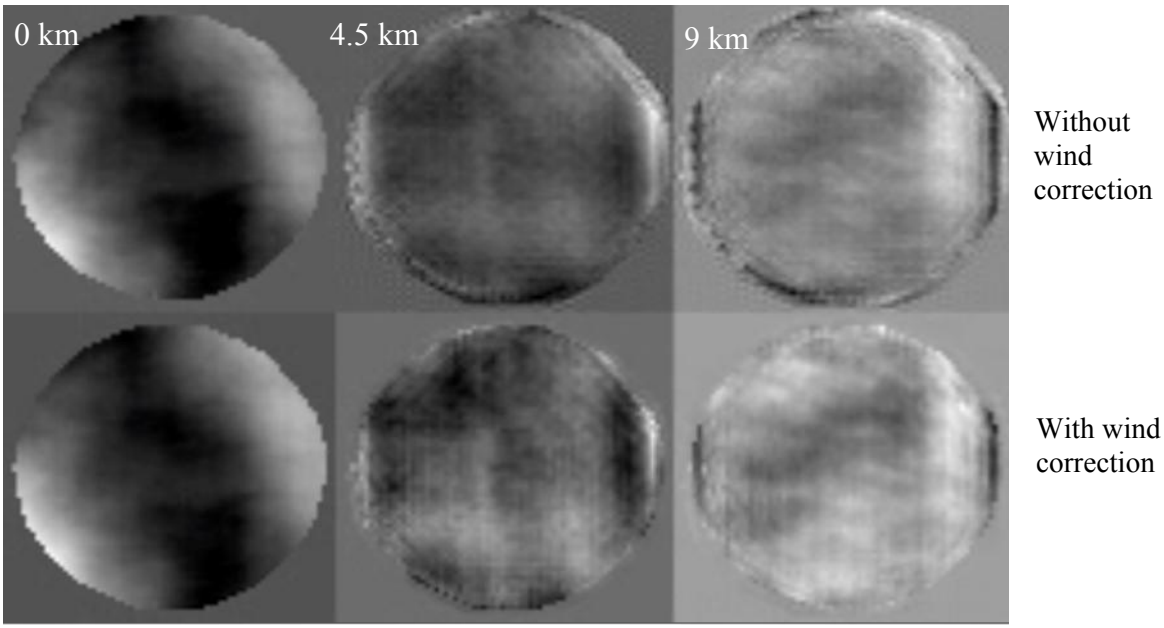

Fig. 6. Comparison of tomographically reconstructed layers of turbulence on the final iteration with wind correction (bottom) and without (top). The leftmost column is the ground layer, the middle column is the 4.5 km layer, and the rightmost column is the highest layer at 9 km.

3.3 Discussion

We find that wind shifts of less than one meter, even of 0.5 meters, are sufficient to lend some improvement to the Strehls. Since this bench has very little photon error, we surmise that wind correction is reducing the tomography error to realize this gain. Although it is clear that the ring of error surrounding the central overlapping metapupil at 9 km is suppressed, it is not certain that this error was originally due to blind modes; it might be due to a registration error or open-loop edge effects. In either case, wind correction provided a good solution in short order.

Typical measured persistence times of shear layers in the integrated atmosphere range between 60 ms and 200 ms, which for low wind speeds of 10 m/s correspond to persistence distances of 0.6-2 meters. Other studies show significantly longer persistence times with improved filtering techniques.[25] IR AO systems, with subaperture sizes on the order of 0.5 m, would not see as much gain as systems with small subapertures. Thus, NGAO and other visible-light AO systems being planned are posed to benefit significantly from wind correction.

4. ACKNOWLEDGEMENTS

This work has been supported by the National Science Foundation Science and Technology Center for Adaptive Optics, managed by the University of California at Santa Cruz under cooperative agreement No. AST - 9876783. S.M.A acknowledges the support of the Allen family through UCO/Lick.

REFERENCES

[1] J. Beckers, "Increasing the size of the isoplanatic patch with multiconjugate adaptive optics," Very Large Telescopes and their Instrumentation, ESO Conference and Workshop Proceedings, March 21-24, 1988, Garching: ESO, 693.

[2] Assemat, F., et al., "FALCON: a new-generation spectrograph with adaptive optics for the ESO VLT," Proc. SPIE 5237, 211-222 (2004).

[3] Hammer, F., et al., "FALCON: a concept to extend adaptive optics corrections to cosmological fields," Proc. SPIE 5382, 727-736 (2004).

[4] Dekany, R., et al., "Adaptive Optics requirements definition for TMT," Proc. SPIE 5490, 879-890 (2004).

[5] Marchetti, E., "On-sky testing of the multi-conjugate adaptive optics demonstrator," The Messenger, vol. 129, p. 8-13 (2007)

[6] Knutsson, P and Owner-Petersen, M, "Emulation of dual-conjugate adaptive optics on an 8-m class telescope," Optics Express, 11, 2231 (2003).

[7] Langlois, M., et al., "Solar multi-conjugate adaptive optics at the Dunn Solar Telescope: preliminary results," Proc. SPIE 5490, 59-66 (2004).

[8] Ragazzoni, R., et al, "Layer-oriented MCAO projects and experiments: an update," 5169, 181-189 (2003).

[9] Gavel, D., et al, "Villages: an on-sky visible wavelength astronomy AO experiment using a MEMS deformable mirror," 6888, 4-7 (2008).

[10] Velur, V., et al, "Multiple guide star tomography demonstration at Palomar observatory," Proc. SPIE 6272, 169 (2006).

[11] Myers, R., et al, "CANARY: The on-sky NGS/LGS MOAO demonstrator for EAGLE", Proc. SPIE, in press (2008).

[12] Wizinowich, P., et al., "W.M. Keck Observatory's next generation adaptive optics facility," Proc. SPIE, in press (2008).

[13] Gavel, D., et al., "Concept for the Keck next-generation adaptive optics system," Proc. SPIE, in press (2008).

[14] Gavel, D., "Tomography for multiconjugate adaptive optics systems using laser guide stars," 5490, 1356-1373 (2004).

[15] Yang, Q., Vogel, C., and Ellerbroek, B., "Fourier domain preconditioned conjugate gradient algorithm for atmospheric tomography," Applied Optics IP 45, 5281-5293 (2006).

[16] Johnson, L., "Wind estimation and prediction for adaptive optics control systems," Proc. SPIE, in press (2008).

[17] Wiberg, D., et al, "Adaptive optics control of wind blown turbulence via translation and prediction," Proc. SPIE 6272, 92 (2006).

[18] Petit, C., et al, “First laboratory demonstration of closed-loop Kalman based optimal control for vibration filtering and simplified MCAO,” Proc. SPIE 6272, 54 (2006).
[19] Ammons, S.M., et al., “First results from the UCSC Laboratory for Adaptive Optics multi-conjugate and multi-object adaptive optics testbed,” Proc. SPIE 6272, 2 (2006).
[20] Ammons, S.M. et al., “Enabling laboratory demonstrations of multi-object adaptive optics with linearity calibrations,” Proc. SPIE 6691, 5 (2007).
[21] Laag, E., et al., Multi-conjugate adaptive optics results from the laboratory for adaptive optics MCAO/MOAO testbed,” JOSA, in press (2008).
[22] L. Gilles, "Closed-loop stability and performance analysis of least-squares and minimum-variance control algorithms for multiconjugate adaptive optics," Appl. Opt. 44, 993-1002 (2005).
[23] A. Tokovinin, M. Le Louarn, and M. Sarazin, “Isoplanatism in a multiconjugate adaptive optics system,” J. Opt. Soc. Am. A 17, 1819–1827 (2000).
[24] Laag, E., et al, “Open-loop woofer tweeter control on the LAO multi-conjugate adaptive optics testbed,” Proceedings of The 6th International Workshop on Adaptive Optics for Industry and Medicine, Ireland (2007).
[25] Poyneer, L., et al., “Towards feasible and effective predictive wavefront control for adaptive optics,” Proc. SPIE, in press (2008).